Title

Multiscale interaction of a tearing mode with drift wave turbulence: A minimal self-consistent model

Journal

Physics of Plasmas, 13(3)

ISSN

1070-664X

Authors

McDevitt, CJ
Diamond, PH

Publication Date

2006-03-01

DOI

10.1063/1.2177585

Multiscale interaction of a tearing mode with drift wave turbulence: A minimal self-consistent model

C. J. McDevitt and P. H. Diamond
Center for Astrophysics and Space Sciences and Department of Physics, University of California at San Diego, La Jolla, California 92093-0424

(Received 20 December 2005; accepted 27 January 2006; published online 10 March 2006)

A minimal self-consistent model of the multiscale interaction of a tearing mode with drift wave turbulence is presented. A tearing instability in a cylindrical plasma interacting with electrostatic drift waves is considered, for reasons of simplicity. Wave kinetics and adiabatic theory are used to treat the feedback of tearing mode flows on the drift waves via shearing and radial advection. The stresses exerted by the self-consistently evolved drift wave population density on the tearing mode are calculated by mean field methods. The principal effect of the drift waves is to pump the resonant low-m mode via a negative viscosity, consistent with the classical notion of an inverse cascade in quasi-two-dimensional turbulence. This process can occur alone or in synergy with current gradient drive of the low-m mode. Speculations of the relation of this multiscale process to the more general issue of the fate of energy transferred to large scales by an inverse cascade are presented. The existence of nonlinearly driven vortices pinned to low-q surfaces as a class of highly anisotropic dissipative structures which terminate the inverse cascade is proposed. The evolution of a finite size magnetic island is discussed. © *2006 American Institute of Physics*. [DOI: 10.1063/1.2177585]

I. INTRODUCTION

Magnetohydrodynamic (MHD) stability continues to be a critical consideration in the design of magnetic confinement devices, especially tokamaks. It has long been known that MHD instabilities can and do limit discharge performance. For example, the low-β current gradient driven disruption is usually explained in terms of the interaction between magnetic islands developing from tearing instabilities. The β limit and the associated high-β disruption are usually associated with pressure gradient driven ballooning or kink modes. In recent years, appreciation of the importance of neoclassical tearing modes (NTMs) has risen considerably. NTMs are driven by the bootstrap current (i.e., produced by the pressure gradient and toroidicity), and result from the interaction of seed currents with parallel and cross-field transport and the resulting feedback loop between the island, the local currents, and the pressure gradient. In simple terms, island induced flattening of the pressure gradient drives further island growth. The details of NTM theory are numerous and a review is far beyond the scope of this paper. The interested reader is referred to Refs. 1–6. However, it is instructive to note that polarization currents and cross-field turbulent transport are *both* thought to be critical to NTM evolution. Since the cross-field transport is driven by ambient microturbulence, and the turbulent advection of vorticity which drives the nonlinear polarization drift also is responsible for generating zonal flows, the statement that *NTM evolution is strongly coupled to the ambient turbulence dynamics* appears irrefutable. Therefore, a successful theory of NTM evolution must treat the low-m island and the high-m, n, and k_r turbulence consistently, and on an equal footing.

The reversed field pinch (RFP) is also a confinement device where the interaction of turbulence with large scale MHD is important. Recently, a spontaneous transition to a quasisingle helicity (QSH) state of good confinement was predicted on the basis of numerical simulations and subsequently observed in experiment. The QSH state is predicted to appear for Hartmann numbers below a critical value, i.e., for $H=1/\sqrt{\nu\eta}<H_{\mathrm{crit}}$,[7,8] where H has been normalized to the Alfvén time and the minor radius of the plasma. However, based on collisional estimates, the Hartmann numbers within existing RFPs are far too large to meet this criteria. Thus, the actual dissipation, especially the viscosity, must have a turbulent origin.

The problems of NTM evolution in tokamaks and evolution of the QSH state in a RFP are both *multiscale problems*, in that *they require treatment over a broad range of disparate space and time scales*. Interestingly, another such problem is drift wave-zonal flow interaction, in which high-$\mathbf{k}$ drift waves drive an $n=0$, $m=0$ zonal flow and, in turn, are regulated by its shear. Either an analytical or computational approach to such multiscale problems requires what is, in effect, a *dynamic subgrid scale model*, which allows feedback of the resolved scales on the unresolved (small) scales. In the case of the NTM, or tearing modes in RFPs, the feedback will be due to:

(1) large scale flow shears, which strain high-$\mathbf{k}$ modes;
(2) large scale mixing (i.e., radial) flows, which modify the turbulence profile; and
(3) modification of the density, temperature, etc., profiles by the large scale mode, which in turn, alters the excitation of turbulence.

Note that reasons (2) and (3) have no counterpart in the zonal flow problem, since flows there are azimuthally symmetric. However, it is again interesting to mention that the "inverse cascade" which drives zonal flow formation is a good example of a process which lies outside the standard ansatz of

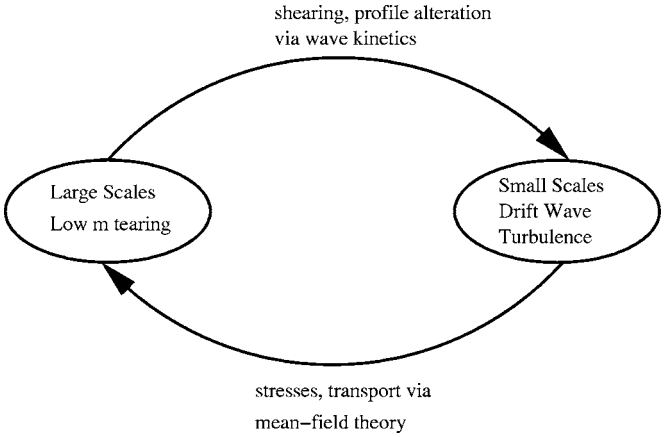

FIG. 1. Minimal multiscale model.

enhanced turbulent dissipation, which forms the underpinning of most subgrid models. Indeed, since *inverse energy transfer is generic to drift wave turbulence*, it is readily apparent that a multiscale model requires more physics content then enhanced dissipation, alone.

It is an understatement to say that the multiscale problem is hideously complicated. Thus, we have sought to further the cause of simplicity by defining the *absolutely minimal working model*, namely that of low-*m* resistive (current gradient driven) tearing evolution in the presence of electrostatic drift wave turbulence in a cylinder (i.e., we will neglect toroidal effects). The tearing mode dynamics are described by reduced MHD (RMHD) and the small scale, large-*m* mode dynamics are described by an *electrostatic fluid model*, such as the Hasegawa-Mima, Hasegawa-Wakatani, or fluid ion temperature gradient (ITG) equations. This minimal model avoids the geometrical complexity of toroidal effects, facilitates analytical progress and physical insight, and permits easy visualization. Moreover, *even further simplification* is made possible by exploiting the disparity in space-time scales between the tearing mode and the background drift waves. In particular, for a tearing mode with wave vector $\mathbf{q}$ [here $\mathbf{q}=(q_x,\ q_\theta,$ and $q_z)$, where q_x is comparable to the inverse layer width and q_θ and q_z are standard notations], and for drift waves with wave vector $\mathbf{k}$, it is the case that $\gamma_q \ll \omega_k$, $q_\theta \ll k_\theta$, and $q_x < k_x$. It is thus apparent that the tearing mode adiabatically modulates the background drift wave population, and the interaction may be treated using a wave kinetic equation (WKE) for the evolution of an adiabatic invariant of the drift wave population. Thus, the minimal model ultimately reduces to:

(1) RMHD for the tearing mode, including the effects of stresses and fluxes driven by the drift waves and
(2) a WKE for $N(\mathbf{k},x,t)$, the drift wave population density proportional to the spectral density. Here N is strained and advected by the tearing mode flows.

Note that albeit simple, the "minimal model" defines a closed self-consistent feedback loop for the interaction of low-*m* MHD and high-$\mathbf{k}$ drift waves. This feedback loop is shown schematically in Fig. 1. Since the drift wave stresses and transport fluxes (directly related to N) evolve in response to straining and mixing by the tearing mode, our minimal model does indeed qualify as a "dynamic subgrid-scale model."

To orient the reader, we think it worthwhile at the outset to survey the physics of multiscale interaction in the minimal model. As noted previously, a critical element of the multiscale problem is the effect of stresses and transport of small scales on large scales. These effects are nearly always the result of quadratic nonlinear interaction, so that schematically:

$$\frac{\partial}{\partial t}L_q \sim \text{linear terms} + \sum_{\mathbf{k}} C_{k,q}A_{k+q}B_{-k},$$

where A and B are amplitudes of small scale modes and $C_{k,q}$ is a coupling coefficient. Here, L_q is the amplitude of the large scale mode. As $|\mathbf{q}| \ll |\mathbf{k}|$, it is natural then to express this interaction in terms of the population density of the small scales. Thus, the equation for L_q may be reexpressed as:

$$\frac{\partial}{\partial t}L_q \sim \text{linear terms} + \sum_{\mathbf{k}} C_{k,q}f(-\mathbf{k})\,\delta N_q(\mathbf{k},t),$$

where $\delta N_q \sim |A_k|^2$ and $B_k = f(\mathbf{k})A_k$. The output of this procedure is a set of "mean field" equations for the low-*m* perturbation in the presence of the high $\mathbf{k}$, ω_k background. Indeed, *the high→low coupling* enters *via the modulation of the high-*$\mathbf{k}$ *background population by the low-m perturbation*. This modulation induces a stress or "pondermotive force" (related to that familiar from Langmuir turbulence) on the low-$\mathbf{k}$ mode.

A largely unexplored element of the multiscale problem is the feedback of large scales on small. This closing of the loop allows the feedback of large→small, which makes the model self-consistent. Use of a wave kinetic equation for N, i.e.,

$$\frac{\partial}{\partial t}N_k + \frac{\partial}{\partial \mathbf{k}}(\omega_k + \mathbf{k}\cdot\mathbf{V})\cdot\frac{\partial}{\partial \mathbf{x}}N_k - \frac{\partial}{\partial \mathbf{x}}(\omega_k + \mathbf{k}\cdot\mathbf{V})\cdot\frac{\partial}{\partial \mathbf{k}}N_k = \gamma_k N_k + C(N_k),$$

where $\mathbf{V}$ is the velocity of the mean field, ω_k is the linear frequency of the drift waves, and $C(N_k)$ is the collisional operator, provides a useful framework for understanding the various feedback loops. Since $q_x \gg q_y$, tearing mode flows are primarily poloidal. Hence, the radially sheared poloidal flows generated by the low-*m* mode will shear and regulate the high-$\mathbf{k}$ turbulence in a manner similar to the way zonal flows regulate drift waves (see Fig. 2). This effect is accounted for by the $\partial/\partial x(k_y V_y)\,\partial N_k/\partial k_x$ term in the wave kinetic equation, which results in amplification of k_x. Note that strong shears can trap background drift waves,[9,10] producing a strongly nonlinear multiscale interaction. Another interesting feedback loop operates via $V_x \partial N_k/\partial x$. This corresponds to tearing-mode induced modification of the turbulence profile. The $V_x \partial N_k/\partial x$ term also accounts for turbulence spreading,[11–13] a process which is potentially important in NTM evolution. Finally, the modifications in ∇P, ∇T, and ∇n induced by the tearing mode can feedback on γ_k, the

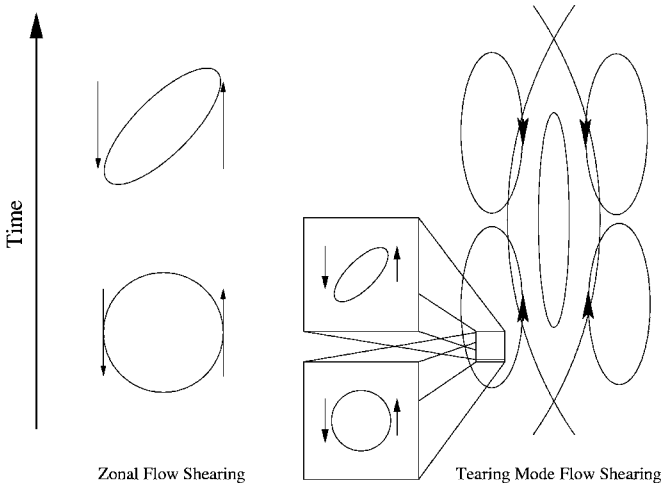

FIG. 2. Zonal shear flows are similar to the shear flows of thin, low-m magnetic islands.

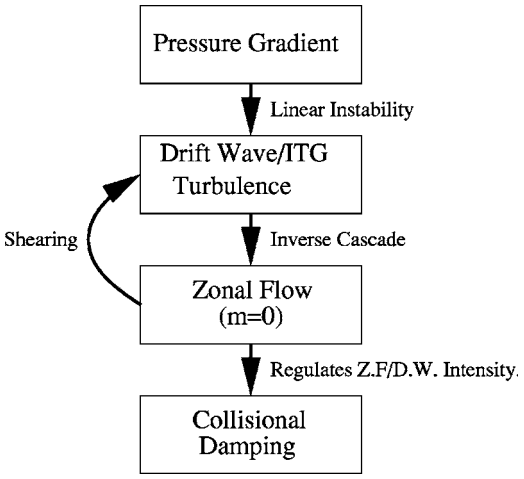

FIG. 3. Schematic of drift wave-zonal flow phenomenon.

local growth or excitation rate for the high-**k** turbulence. It is interesting to note that low→high feedback occurs in both **k** space (via shearing) and position space (via radial mixing). These two processes can act synergistically, as well.

We note here that the problem of how a tearing mode interacts with background turbulence is one with a long, albeit intermittent, history in magnetic fusion theory. Most of the previous attempts have focused on a search for anomalous dissipation in the Ohm's Law, such as a turbulent electron viscosity[14–16] or resistivity.[17] The hope here was to find a dissipation mechanism which was robust in the limit of small collisional resistivity. These models all focused on nonlinearities in Ohm's Law, did not consider feedback on the ambient micro turbulence, and so were not self-consistent. Other studies have considered the effect of incoherent emission from high-**k** modes as a "trigger" for (Ref. 18) or a means of "accelerating" (Ref. 19) the linear growth of low m. Neither of these studies treated feedback self-consistently. However, we wish to emphasize that incoherent emission effects are potentially important and merit further study. Ongoing research strongly suggests that incoherent emission from higher harmonics can substantially accelerate the growth of low-m NTMs.

In this article, then, we present a minimal model of multiscale interaction between high-**k** drift waves and a low-m tearing mode in a cylinder. The basic model is set forth and mean field equations for the low-m dynamics are derived. The wave-kinetic equation for the drift wave population density is presented and discussed, and the key physics of the high-$\mathbf{k} \rightleftharpoons$ low-m feedback loops is elucidated. We study the stability, scales and growth rates of both a low-m electrostatic vortex mode and a low-m tearing mode, with $\Delta' > 0$. The key small scale→large scale effect (for the case of electrostatic turbulence) is a negative turbulent viscosity. For realistic parameters, this effect dominates inertia, and thus (along with field line bending) sets the scale of the tearing layer. Outgoing wave boundary conditions are imposed in order to control the rapid oscillations induced by the negative viscosity. In contrast to most cases in MHD, a real frequency is also induced. We also sketch an outline of the "Rutherford" calculation for the case of a finite size island. The meaning and interpretation of the Rutherford theory in the presence of self-consistently evolving background turbulence are discussed. Again we emphasize that this analysis corresponds to a minimal model, hence effects such as incoherent emission, toroidal effects, finite β microturbulence, spatial dynamics of the turbulence spectrum, i.e., turbulence spreading, turbulent heat transport, self-consistent evolution of temperature and density profiles with island, etc., will not be treated.

The remainder of this article is organized as follows: In Sec. II we discuss the general multiscale formulation of the problem. In Sec. III we present a linear theory of the tearing instability in the presence of a negative viscosity. Finally, Sec.IV contains the conclusions and a discussion of broader issues and future work.

II. FORMULATION

A. Wave kinetics for small scale drift waves

As shown in Refs. 20 and 21 for the case of drift wave-zonal flow systems, wave kinetics is a useful formalism for studying modulational instabilities. Zonal flows induce a nonlinear frequency shift in the wave kinetic equation via a Doppler shift, and modulation of the diamagnetic drift velocity. The modulation of the drift wave turbulence *by* the zonal flow reacts back *on* the zonal flow through the polarization nonlinearity. This can be shown to lead to a nonlocal transfer of energy *from* the drift waves *to* the zonal flow, thus amplifying the initial shear perturbation. A schematic flow chart of the drift wave-zonal flow system is given in Fig. 3.

In this work we will be focusing on low $m \neq 0$ modes, for which the above-mentioned picture is somewhat modified. For the case of a low-m tearing mode, both the inverse cascade and the current gradient (via the tearing mechanism) can drive large scale flow. Also, the backreaction on the drift wave turbulence is more complex. Aside from shearing the drift wave turbulence as in the case of zonal flows, a low-m tearing mode will react back on the turbulence both by modifying the pressure profile (flattening the pressure gradient

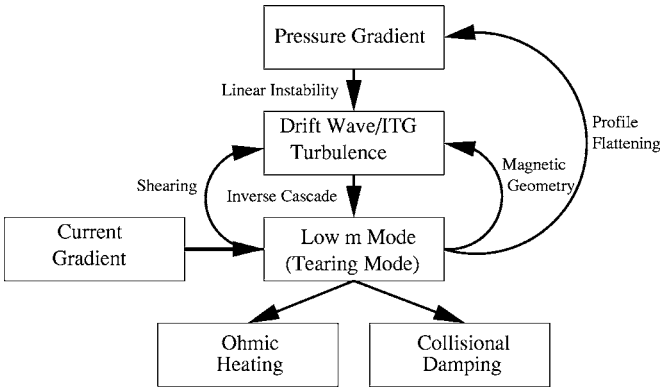

FIG. 4. Schematic of low-m mode interaction with drift wave turbulence.

inside the island and potentially steepening it outside), and perturbing the magnetic field topology, thus modifying the effective local magnetic shear. The structure of the high-$\mathbf{k}$ turbulence should be calculated in the evolving magnetic geometry which incorporates the island. A schematic flow chart of the low-m tearing mode interaction with drift wave turbulence is given in Fig. 4.

In order to derive a WKE for the small scales, it is useful to first identify a quantity which varies adiabatically. One might expect an adiabatic invariant such as wave action, of the form $N_k = E_k/\omega_k$. However, as was shown in Refs. 22 and 23, the *actual* adiabatic invariant for a drift wave system in the presence of mean flows is $N_k = (1+\rho_s^2 k_\perp^2)^2 |\phi_k^>|^2$. This quantity can be recognized as the drift wave potential enstrophy, which is a measure of the vorticity density associated with the drift waves. Note however, for zonal flows, with $k_\theta = 0$, the wave action and potential enstrophy are identical. We note in passing that, similar to the two-dimensional (2D) Euler equation, the Hasegawa-Mima equation corresponds to a law of conservation of potential vorticity along fluid trajectories. Thus, it is not surprising that the "adiabatic invariant" is the potential enstrophy. However, in contrast to the Hasegawa-Mima equation, the 2D Euler equation possesses no "waves." This observation could lead one to conclude that a description of incompressible 2D hydrodynamic turbulence via a WKE is impossible, since their are no "wave quanta." However, as shown by Ref. 23, a WKE can be derived from the 2D Euler equation, where in this limit, the adiabatic invariant is the enstrophy density which can be interpreted as the "roton" number density.

Proceeding with the derivation of the WKE, it is convenient to separate the fields into a large scale, mean field piece $\phi_k^<$, plus a small scale fluctuation $\phi_k^>$, separated by a cutoff scale $|\mathbf{k}_c|$. Applying this scale separation procedure, an equation for the microturbulence, which is similar to the Hasegawa-Mima equation,[24] but retains the mean field contribution, can be written as

$$0 = \left(\frac{\partial}{\partial t} + \frac{c}{B_0}(\hat{\mathbf{z}} \times \nabla\phi^<)\cdot\nabla\right)\frac{e\phi^>}{T_e} + v_e^* \frac{\partial}{\partial y}\frac{e\phi^>}{T_e} - \rho_s^2\left(\frac{\partial}{\partial t} + \frac{c}{B_0}(\hat{\mathbf{z}} \times \nabla\phi^<)\cdot\nabla\right)\nabla_\perp^2 \frac{e\phi^>}{T_e}. \quad (1)$$

Here, $\rho_s = c_s/\omega_{ci}$, $c_s = \sqrt{T_e/m_i}$, $v_e^* = cT_e/(eB_0L_n)$ is the electron diamagnetic drift velocity, and $\hat{z}$ is in the direction of the mean magnetic field. We are primarily interested in investigating the nonlocal interaction of drift waves with large scale, low-m modes. Hence, local interactions between drift waves, i.e., the quadratic nonlinearities in $\phi^>$, have been dropped. Local interactions will be introduced later via the insertion of a phenomenological collisional operator in the Boltzmann equation for the wave quanta density. Also, note the addition of an advective term representing the large scale mean flow.

Exploiting the scale separation and averaging over the fast scales, a WKE for the evolution of the drift wave potential enstrophy density in the presence of a weakly varying background can be written (see Ref. 22 for details)

$$\frac{\partial}{\partial t}N_k + \frac{\partial}{\partial \mathbf{k}}(\omega_k + \mathbf{k}\cdot\mathbf{V}_0)\cdot\frac{\partial}{\partial \mathbf{x}}N_k - \frac{\partial}{\partial \mathbf{x}}(\omega_k + \mathbf{k}\cdot\mathbf{V}_0)\cdot\frac{\partial}{\partial \mathbf{k}}N_k = S, \quad (2)$$

where

$$\omega_k = \frac{v_e^* k_y}{1+\rho_s^2 k_\perp^2}, \quad \mathbf{V}_0 = \frac{c}{B_0}(\hat{\mathbf{z}} \times \nabla\phi^<),$$

$$N_k = (1+\rho_s^2 k_\perp^2)^2 I_k.$$

Here N_k is the enstrophy density, I_k is a Wigner function defined as $I_k = \int d\mathbf{q} e^{i\mathbf{q}\cdot\mathbf{x}} \langle \phi_{k+q}^> \phi_{-k}^> \rangle$, and the angular brackets represent an average over the small, rapidly varying scales. The second term on the left-hand side in Eq. (2) corresponds to the advection term with a Doppler shift due to the mean flow. Here the "mean flow" is the flow associated with the MHD mode. The third term describes the refraction of the drift waves as a result of any spatial dependence of the real frequency (i.e., spatial variations of the density gradient), and through the weak spatial variation of the mean field. Notice that in the absence of the source term S, this amounts to the conservation of wave quanta number N_k along ray trajectories. The source term S can be symbolically written as $S = \gamma_k N_k - \Delta\omega_k N_k^2$. The first term corresponds to the linear drive of the drift waves, which should be computed *in the presence of the tearing mode*. This is necessary since the island will modify both the local profiles and the drift wave mode structure. The second term corresponds to the nonlinear like-scale interaction. In the absence of the nonconservative source term, Eq. (2) is isomorphic to the Vlasov equation, and thus provides a particularly convenient description of the intensity field of the drift wave turbulence.

B. Mean field equations for large scale tearing mode

In the previous section we introduced a wave kinetic formulation which allowed us to describe the development of the drift wave turbulence in terms of an adiabatically varying wave population density N_k. This approach enables us to develop a *dynamic subgrid scale* model for drift wave-MHD interaction. This model is "dynamic" since there is feedback, via shearing and modulation, by the large scale flows on the small scale turbulence, which exerts a stress on it. We are now interested in a description of the mean field (i.e., tearing

mode) equations in the presence of the background micro turbulence. We describe the MHD fields at low m via RMHD. This description ignores a number of effects that become important in the low collisionality, high temperature regime. However, it constitutes the absolute minimal description of unstable tearing mode dynamics. Further, as has been observed in drift wave-zonal flow systems, the background turbulence behaves as a source of energy for the large scales, and drives mean flows via the stress term. Thus, we seek to understand how the inclusion of this external drive affects the evolution of the tearing mode. For this reason, it will be convenient to begin with as simple a description as possible. The RMHD equations are given by

$$0 = \frac{\partial}{\partial t}\psi + \frac{c}{B_0}(\hat{\mathbf{z}} \times \nabla\phi) \cdot \nabla\psi - v_A \frac{\partial}{\partial z}\phi - \eta_c \nabla_\perp^2 \psi, \tag{3}$$

$$0 = \frac{\partial}{\partial t}\nabla_\perp^2 \phi + \frac{c}{B_o}(\hat{\mathbf{z}} \times \nabla\phi) \cdot \nabla\nabla_\perp^2 \phi - v_A \frac{\partial}{\partial z}\nabla_\perp^2 \psi - \frac{c}{B_0}(\hat{\mathbf{z}} \times \nabla\psi) \cdot \nabla\nabla_\perp^2 \psi - \nu_c \nabla_\perp^2 \nabla_\perp^2 \phi. \tag{4}$$

Here ψ is normalized to v_A/c, and the Alfvén velocity is defined as $v_A = B_0/\sqrt{4\pi}$, where ρ_0 has been set equal to one. Since the small scales are described by an electrostatic model, small scale magnetic perturbations are neglected. Thus, the stream function and flux function can be written as $\phi = \phi^< + \phi^>$, $\psi = \psi^<$. Substituting these definitions into Eqs. (3) and (4) and averaging, gives the large scale equations:

$$0 = \frac{\partial}{\partial t}\psi^< + \frac{c}{B_0}(\hat{\mathbf{z}} \times \nabla\phi^<) \cdot \nabla\psi^< - v_A \frac{\partial}{\partial z}\phi^< - \eta_c \nabla_\perp^2 \psi^<, \tag{5}$$

$$0 = \frac{\partial}{\partial t}\nabla_\perp^2 \phi^< + \frac{c}{B_0}(\hat{\mathbf{z}} \times \nabla\phi^<) \cdot \nabla\nabla_\perp^2 \phi^< - v_A \frac{\partial}{\partial z}\nabla_\perp^2 \psi^< - \frac{c}{B_0}(\hat{\mathbf{z}} \times \nabla\psi^<) \cdot \nabla\nabla_\perp^2 \psi^< - \nu_c \nabla_\perp^2 \nabla_\perp^2 \phi^< + \frac{c}{B_0}\langle(\hat{\mathbf{z}} \times \nabla\phi^>) \cdot \nabla\nabla_\perp^2 \phi^>\rangle. \tag{6}$$

Note the absence of a stress term within the induction equation. This precludes the appearance of a turbulent resistivity. As considered in Refs. 21 and 25, electrostatic fluctuations can generate an anomalous resistivity through the $\langle \tilde{n}\tilde{E}_\parallel \rangle$ term. This anomalous resistivity can be calculated by modulating the parallel acceleration term with respect to $\psi^<$, which can be written symbolically as $\delta\langle \tilde{n}\tilde{E}_\parallel \rangle \sim \Sigma_k C_k (\delta N_k/\delta\psi^<)\psi^<$. However, in this simple model for electrostatic drift waves [as can be seen from Eq. (2)], N_k is unaffected by perturbations in $\psi^<$ ($\delta N_k/\delta\psi^< = 0$). This is a consequence of assuming that drift waves and Alfvén waves decouple, which is valid only in a low beta plasma. In the finite beta regime, perturbations of $\psi^<$ would enter into the WKE by bending the mean magnetic field lines, and then modulating the frequency of the drift-Alfvén modes as discussed in Ref. 26. Just as the negative viscosity excites low-m flows which are similar to zonal flows, this effect could drive a low-m magnetic field similar to a zonal field. Also, note that for a large magnetic island, the effective magnetic shear at the X point differs substantially from that of the O point. Thus, for large magnetic perturbations, $\psi^<$ would modulate N_k through modifications of the local magnetic shear leading to $\delta N_k/\delta\psi^< \neq 0$, and so produce a turbulent resistivity. However, for the present "minimalist" study we will not consider this possibility.

The simple averaging procedure employed previously, reduces the system into a set of resolved equations for the large scales, and a population density equation for the unresolved small scales. However, although the phase information of small scale fluctuations is averaged out, the evolution of the intensity $N_k \sim \langle \phi_k^> \phi_{-k}^> \rangle$ evolves dynamically via modulations by the large scale mean field. Thus, Eqs. (2), (5), and (6) provide a minimal self-consistent description of the drift wave-tearing mode system.

C. Closure of drift wave-tearing mode system

In order to close the drift wave-tearing mode system, it is necessary to explicitly write the Reynolds stress term within the RMHD equations in terms of the drift wave enstrophy. After integrating by parts twice, the Reynolds stress $\langle(\hat{\mathbf{z}} \times \nabla\phi^>) \cdot \nabla\nabla_\perp^2 \phi^>\rangle$ can be written

$$\begin{aligned}\langle(\hat{\mathbf{z}} \times \nabla\phi^>) \cdot \nabla\nabla_\perp^2 \phi^>\rangle(\mathbf{x},t) &= -\left(\frac{\partial^2}{\partial x^2} - \frac{\partial^2}{\partial y^2}\right)\left\langle \frac{\partial\phi^>}{\partial x}\frac{\partial\phi^>}{\partial y}\right\rangle(\mathbf{x},t) \\ &\quad + \frac{\partial^2}{\partial x\,\partial y}\left[\left\langle\left(\frac{\partial\phi^>}{\partial x}\right)^2\right\rangle(\mathbf{x},t) - \left\langle\left(\frac{\partial\phi^>}{\partial y}\right)^2\right\rangle(\mathbf{x},t)\right],\end{aligned} \tag{7}$$

where we have written the angular brackets in the form $\langle\ldots\rangle(\mathbf{x},t)$, to emphasize that the averages are over the fast spatial and temporal scales, such that a slow spatial and temporal dependence remains. After Fourier transforming, the stress terms can be rewritten in terms of the drift wave enstrophy density:

$$\begin{aligned}\langle(\hat{\mathbf{z}} \times \nabla\phi^>) \cdot \nabla\nabla_\perp^2 \phi^>\rangle(\mathbf{x},t) &= -\left(\frac{\partial^2}{\partial x^2} - \frac{\partial^2}{\partial y^2}\right)\int d\mathbf{k}\frac{k_x k_y}{(1+\rho_s^2 k_\perp^2)^2}N_k(\mathbf{x},t) \\ &\quad + \frac{\partial^2}{\partial x\,\partial y}\int d\mathbf{k}\frac{(k_x^2 - k_y^2)}{(1+\rho_s^2 k_\perp^2)^2}N_k(\mathbf{x},t).\end{aligned} \tag{8}$$

From this expression it is clear that for isotropic turbulence, both integrals vanish. Thus, a necessary condition for a finite contribution to the mean field vorticity equation from the background drift wave turbulence is either anisotropy of the equilibrium drift wave spectrum, or a "seed" asymmetry, which arises from the large scale mean fields which modulate the drift wave spectrum. The latter is the subject of the present discussion, as we are concerned with tearing interaction with the ambient drift wave turbulence.

Considering small deviations from the equilibrium drift wave spectrum N_k^0 (i.e., seed asymmetries), Eq. (2) can be

linearized for small perturbations of the form $(\delta N_k, \phi^<) \sim e^{i\mathbf{q}\cdot\mathbf{x}-i\omega_q t+\gamma_q t}$, yielding an expression for the response of the drift waves to the tearing mode field:

$$\delta N_k = \frac{c}{B_0}\frac{-1}{(\omega_q - \mathbf{q}\cdot\mathbf{v}_{\mathrm{gr}}) + i(\gamma_q+\gamma_k)} \times\left\{ q_y\frac{\partial N_k^0}{\partial x} - i(\mathbf{k}\times\mathbf{q})_z\mathbf{q}\cdot\frac{\partial N_k^0}{\partial \mathbf{k}}\right\}\phi^<. \tag{9}$$

Here, ω_q and γ_q correspond to the real frequency and growth rate of the MHD mode, respectively, and are assumed slow in comparison to the ambient drift wave turbulence, γ_k is the linear growth rate of the drift wave turbulence, and $\mathbf{v}_{\mathrm{gr}} = \partial\omega_q/\partial\mathbf{k}$. It is useful at this point to compare the magnitudes of the two terms in curly braces. Estimating their magnitudes as $q_y\partial N_k^0/\partial x \sim N_k^0(q_y/L_I)$ and $(\mathbf{k}\times\mathbf{q})_z\mathbf{q}\cdot\partial N_k^0/\partial\mathbf{k}\sim q_x^2 N$, where L_I corresponds to the length scale on which the turbulence profile varies in space, we find that for $q_x^2 > q_y/L_I$ the first term in curly braces can be neglected. This inequality is virtually always satisfied, except perhaps at a transport barrier. Thus, we are motivated to focus purely on the k space dynamics induced by shearing (the second term in curly braces). However, we note that $\partial N_k^0/\partial x$-driven contributions to δN_k may enter with a phase $\pi/2$ different from $\partial N_k^0/\partial\mathbf{k}$-driven contributions. These may contribute effects which are structurally similar to the diamagnetic terms. As we have neglected even standard diamagnetic effects in this article, we leave these more exotic analyses to future work. Also, notice that the above-mentioned linearization is purely for convenience. Though the WKE (naively) appears to be nonlinear, it is actually bilinear (ignoring the collision operator), so that even for strong modulation fields, the response of N_k may be calculated by the method of characteristics. Physically, such strong modulations can cause trapping of drift waves in the island flows. Substituting Eq. (9) into the polarization drift term of the vorticity equation [Eq. (8)] gives to lowest order

$$\begin{aligned}\langle(\hat{\mathbf{z}}\times\nabla\phi^>)\cdot\nabla\nabla_\perp^2\phi^>\rangle =& -c_s^2\int d\mathbf{k}\frac{\rho_s^2k_y^2}{(1+\rho_s^2k_\perp^2)^2}\frac{\gamma_k}{(\gamma_k^2+(\mathbf{q}\cdot\mathbf{v}_{gr})^2)}k_x\frac{\partial N_k^0}{\partial k_x}\frac{\partial^4\phi^<}{\partial x^4}\\ &-c_s^2\int d\mathbf{k}\frac{\rho_s^2k_x^2}{(1+\rho_s^2k_\perp^2)^2}\frac{\gamma_k}{(\gamma_k^2+(\mathbf{q}\cdot\mathbf{v}_{gr})^2)}k_y\frac{\partial N_k^0}{\partial k_y}\frac{\partial^4\phi^<}{\partial y^4}+c_s^2\int d\mathbf{k}\frac{\rho_s^2}{(1+\rho_s^2k_\perp^2)^2}\frac{\gamma_k}{(\gamma_k^2+(\mathbf{q}\cdot\mathbf{v}_{gr})^2)}\\ &\times\left(k_x^3\frac{\partial N_k^0}{\partial k_x}+k_y^3\frac{\partial N_k^0}{\partial k_y}\right)\frac{\partial^2}{\partial x^2}\frac{\partial^2\phi^<}{\partial y^2}\\ =& -\nu_{xx}\frac{\partial^4\phi^<}{\partial x^4}-\nu_{yy}\frac{\partial^4\phi^<}{\partial y^4}+\nu_{xy}\frac{\partial^2}{\partial x^2}\frac{\partial^2\phi^<}{\partial y^2},\end{aligned} \tag{10}$$

Inserting these expressions into the large scale vorticity equation yields

$$\begin{aligned}0 =& \frac{\partial}{\partial t}\nabla_\perp^2\phi^< + \frac{c}{B_0}(\hat{\mathbf{z}}\times\nabla\phi^<)\cdot\nabla\nabla_\perp^2\phi^< - v_A\frac{\partial}{\partial z}\nabla_\perp^2\psi^<\\ &-\frac{c}{B_0}(\hat{\mathbf{z}}\times\nabla\psi^<)\cdot\nabla\nabla_\perp^2\psi^< - \nu_{xx}\frac{\partial^4}{\partial x^4}\phi^< - \nu_{yy}\frac{\partial^4}{\partial y^4}\phi^<\\ &+\nu_{xy}\frac{\partial^2}{\partial x^2}\frac{\partial^2}{\partial y^2}\phi^<.\end{aligned} \tag{11}$$

Here the collisional viscosity has been dropped, since it is, in general, negligible compared to the turbulent viscosity. The stress terms (i.e., the last three terms on the right-hand side of the vorticity equation) have the form of an "anomalous" or "turbulent" viscosity. Note that for $k_x\partial N_k^0/\partial k_x < 0$ (i.e., $N_k^0 \sim |k|^{-\alpha}$, which is observed in all studies and predicted by all models of drift wave turbulence), the value of ν_{xx} (the dominant term for the tearing mode ordering $\partial/\partial x \gg \partial/\partial y$, which applies on large scales), will be *negative*. The presence of a negative viscosity on large scales due to nonlocal interactions with the background micro turbulence is a result familiar from considerations of drift wave-zonal flow systems. In simple terms, it is a consequence of the fact that in 2D (here the strong B_0 enforces quasi-two dimensionality), fluid kinetic energy tends to inverse cascade (producing large scale growth), rather than forward cascade which, produces dissipation at large scales. However, our purpose in emphasizing the result here is that with one exception,[18] there has been very little effort put into investigating the impact of a turbulent source on tearing mode physics. Also, Ref. 18 did not self-consistently treat the backreaction of large scales on small scales.

We estimate the magnitude of the anomalous viscosity, using a mixing length argument. Mixing length arguments usually constitute a rough upper limit on the saturated intensity of the background turbulence, which is useful for obtaining a rough scaling for diffusion coefficients. In essence, mixing length arguments correspond to balancing the nonlinear advection of a quantity (say density) with the linear drive (generally a gradient in a mean quantity) for the system. Schematically:

$$\tilde{\mathbf{v}} \cdot \nabla \tilde{n} \sim \tilde{v}_x dn_0/dx \Rightarrow \tilde{n}/n_0 \sim l/L_n,$$

where l is the mixing length. Self-consistent feedback on intensity (via predator-prey models) will be considered in the future. For drift waves, we can approximate $e\phi^{>}/T_e \sim 1/(k_\perp L_n)$, where L_n is the perpendicular length scale over which the density varies. The magnitude of the turbulent viscosity can then be estimated to be $|\nu_{xx}| \approx (c_s^2/\gamma_k) 1/k_\perp^2 L_n^2 \approx (c_s^2/\gamma_k)\rho_s^2/L_n^2$, where we have used ρ_s to estimate the mixing length. Finally, estimating the linear drift wave growth rate to be of the order of the drift wave linear frequency, $\gamma_k \approx v_e^* k_y \approx c_s/L_n$, yields an estimate of the turbulent viscosity as $|\nu_{xx}| \approx (\rho_s/L_n)\omega_{ci}\rho_s^2 \sim D_{\mathrm{GB}}$. Here D_{GB} denotes the gyro-Bohm diffusivity, which is far in excess of the ion-ion collisional viscosity ρ_i^2/τ_{ii}, or the neoclassical viscosity. To estimate the relative sizes of the turbulence driven flux and linear inertia, we compare $\nu_{xx} \sim D_{\mathrm{GB}}$ with $\gamma_T x_T^2$, where γ_T and x_T are the usual tearing mode growth rate and linear layer width, respectively. A simple calculation yields the conclusion that turbulent stresses will exceed inertia for

$$D_{\mathrm{GB}} > \frac{a^2}{\tau_\eta}(\Delta' a)^{6/5}(1/S)^{2/5}(L_s/am)^{2/5}. \tag{12}$$

Here $S = \tau_\eta/\tau_A$, where $\tau_\eta^{-1} = \eta/a^2$ and $\tau_A^{-1} = v_A/a$. This expression can be rewritten as $(\omega_{ci}\tau_\eta)(\rho_s/a)^2 > (L_s/\rho_s) \times (1/S)^{2/5}(L_s/am)^{2/5}(\Delta' a)^{6/5}$. For Lundquist numbers on the order of $S \sim 10^5 - 10^7$ and a resistive time scale of $\omega_{ci}\tau_\eta \sim 10^{10} - 10^{12}$, this condition will nearly always be satisfied. Thus, in practical terms, the turbulent stresses *always* exceed inertia. Hence, the turbulent Reynolds stress is seen to be the *dominant microscopic* effect on the large scales.

Note that the above-mentioned analysis has been done for the case of homogeneous micro turbulence. In Appendix B we extend this analysis for the case of ITG turbulence in an RFP, where strong magnetic shear will significantly alter the radial mode structure of the microturbulence. Similar to the previous analysis, a strong nonlocal transfer of energy from the small scale microturbulence to the large scale MHD modes is found for modes with q_y significantly smaller than q_x. This result is in qualitative agreement with Eq. (11) for modes with $\partial/\partial x \gg \partial/\partial y$, which is the relevant tearing mode ordering.

III. LINEAR THEORY OF THE TEARING INSTABILITY IN THE PRESENCE OF A NEGATIVE TURBULENT VISCOSITY

The negative turbulent viscosity derived previously has a magnitude far in excess of the collisional viscosity present within typical plasmas. Further, for the universally observed case where $k_x(\partial N_k^0/\partial k_x) < 0$, the turbulent viscosity will be *negative*, such that energy is fed to the large scales. In considering the effect of a negative viscosity on tearing modes and magnetic islands, it is instructive to first consider the form of the RMHD equations near the resonant surface. Considering perturbations of the form $f(\vec{x},t) = f(x)e^{iq_y y + \gamma_q t}$, Eqs. (11) and (3) can be linearized to give

$$\gamma_q \frac{\partial^2 \phi^<}{\partial x^2} = iq_y v_A \frac{x}{L_s} J + \nu_{xx}\frac{\partial^4 \phi^<}{\partial x^4}, \tag{13}$$

$$\eta_c J = \gamma_q \psi^< - iq_y v_A \frac{x}{L_s}\phi^<, \tag{14}$$

where J is the parallel current, L_s is the shear length, $x = r - r_{m,n}$, and $r_{m,n}$ is the m,n rational surface. Also, since we are considering modes strongly localized around the resonant surface, we have applied the ordering $\partial/\partial x \gg \partial/\partial y$. In the limit in which the inverse growth rate of the tearing mode is long in comparison to the skin time of the resistive layer ($\tau \sim \delta^2/\eta_c$ where δ is the width of the resistive layer), ψ can be assumed to be constant. Making use of this approximation and substituting Eq. (14) into Eq. (13) yields:

$$-\nu_{xx}\frac{\partial^4 \phi^<}{\partial x^4} + \gamma_q \frac{\partial^2 \phi^<}{\partial x^2} = \frac{q_y^2 v_A^2}{\eta_c}\frac{x^2}{L_s^2}\phi^< + i\gamma_q \frac{q_y v_A}{\eta_c}\frac{x}{L_s}\psi_0. \tag{15}$$

From Eq. (15) three regimes can be distinguished: First, in the limit of weak viscosity $|\nu_{xx}| \ll \gamma_T \delta^2$, the viscous term can be dropped and the system reduces to that treated by Ref. 27. In the opposite limit, for which $|\nu_{xx}| \gg \gamma_T \delta^2$, Eq. (15) reduces to the viscosity dominated limit, which was analyzed for the positive viscosity case by Refs. 28 and 29. Finally, an electrostatic limit can also be distinguished ($\psi_0 = 0$). This regime describes an electrostatic vortex driven by an inverse cascade of energy to low but finite m, where resistive field line bending ultimately limits the vortex size.

The first regime will, of course, be largely unaffected by the presence of a negative viscosity. The second regime corresponds to the familiar reconnecting mode. However, for a viscosity induced by drift wave turbulence, the dynamics will be significantly altered. Aside from the free energy resulting from current gradient relaxation, on the large scales, relevant for a low-m tearing mode, the background microturbulence will also act to drive flows nonlinearly, introducing a second channel for the excitation of the large scales. Also, since the background turbulence is ultimately pressure driven, it thus can be said that the inverse cascade couples low-m, resonant excitations to the pressure gradient, *regardless of curvature*.

The third regime consists of a purely electrostatic vortex mode, more akin to a zonal flow, except with a finite k_θ ($m \neq 0$, $n \neq 0$). The primary consequence of the finite poloidal wave number is the introduction of resistive field line bending, which will limit the width of the vortex mode. Also, since this mode is purely electrostatic, it does not involve any reconnection of the magnetic field. This vortex mode merits an independent discussion however, in order to clarify the effect of the negative viscosity on the tearing mode. Moreover, this type of dissipative mode is a possible type of "dissipative structure" for the inverse cascade, i.e., the ultimate repository of the energy transferred to large scales.

A. Electrostatic vortex mode

To clarify the dynamics of the interaction of the inverse cascade with low-m, large scale modes, first consider a purely electrostatic vortex mode excited by negative viscosity. In contrast to a reconnecting mode, which couples to the exterior solution via Δ', the vortex mode[17,30] is a strongly

localized mode which is ∇P driven via the inverse cascade initiated by the background turbulence. Setting $\psi_0=0$, Eq. (15) reduces to

$$|\nu_{xx}|\frac{\partial^4\phi^<}{\partial x^4}+\gamma_q\frac{\partial^2\phi^<}{\partial x^2}=\frac{q_y^2v_A^2}{\eta_c}\frac{x^2}{L_s^2}\phi^<. \tag{16}$$

In order to lower the order of Eq. (16), it is convenient to introduce the Fourier transform with respect to x defined by $\phi^<(q_x)=\int_{-\infty}^{\infty}dxe^{-iq_xx}\phi(x)$, so

$$0=\frac{q_y^2v_A^2}{\eta_c}\frac{1}{L_s^2}\frac{d^2\phi(q_x)}{dq_x^2}+|\nu_{xx}|q_x^4\phi(q_x)-\gamma_qq_x^2\phi(q_x). \tag{17}$$

A closed form analytic solution to this equation is not available. However, a quadratic variational form can be straightforwardly written as

$$-\gamma_q[\phi]=\frac{\int_{-\infty}^{\infty}dq_x\left(\frac{q_y^2v_A^2}{\eta_c}\frac{1}{L_s^2}\left(\frac{d\phi}{dq_x}\right)^2-|\nu_{xx}|q_x^4\phi^2\right)}{\int_{-\infty}^{\infty}dq_xq_x^2\phi^2}. \tag{18}$$

Here, the second term in parentheses corresponds to excitation due to the inverse cascade of energy which drives the low-m cell. The first term is the resistively modified field line bending term, which is stabilizing.

In order to construct a trial function, it is useful to consider Eq. (17) in various limits. Considering first the case of large q_x, Eq. (17) can be written

$$0=\frac{q_y^2v_A^2}{\eta_c}\frac{1}{L_s^2}\frac{d^2\phi_{es}(q_x)}{dq_x^2}+|\nu_{xx}|q_x^4\phi_{es}(q_x). \tag{19}$$

This equation can easily be solved yielding solutions of the form

$$\phi_{es}(q_x)=A\sqrt{q_x}J_{1/6}\left(\frac{x_\nu^3q_x^3}{3}\right)+B\sqrt{q_x}Y_{1/6}\left(\frac{x_\nu^3q_x^3}{3}\right), \tag{20}$$

where $x_\nu=(\eta_c|\nu_{xx}|)^{1/6}(L_s/q_yv_A)^{1/3}$. In the opposite limit, for small values of q_x, Eq. (17) reduces to

$$0=\frac{q_y^2v_A^2}{\eta_c}\frac{1}{L_s^2}\frac{d^2\phi_{es}(q_x)}{dq_x^2}-\gamma_qq_x^2\phi_{es}. \tag{21}$$

The general solution for Eq. (21) is given by

$$\phi(q_x)=C\sqrt{q_x}I_{1/4}\left(\frac{x_T^2q_x^2}{2}\right)+D\sqrt{q_x}K_{1/4}\left(\frac{x_T^2q_x^2}{2}\right), \tag{22}$$

where $x_T=(\eta_c\gamma_q)^{1/4}(L_s/(v_Aq_y))^{1/2}$. When $|\nu_{xx}|q_x^4\approx\gamma_qq_x^2$, $\phi(q_x)$ can be expressed approximately as

$$\phi(q_x)\approx E\mathrm{Ai}(-\alpha(q_x-q_c))+F\mathrm{Bi}(-\alpha(q_x-q_c)), \tag{23}$$

where $\alpha=2^{1/3}\eta_c^{1/3}\gamma_q^{1/2}/|\nu_{xx}|^{1/6}(L_s/q_yv_A)^{2/3}$, $q_c=\sqrt{\gamma_q/|\nu_{xx}|}$, and Ai, Bi are Airy functions of the first and second kind, respectively. Since Eq. (20) resulted from balancing the second order derivative with the $q_x^4\phi$ term, introduction of $\phi(q_x)$ as given by Eq. (20) makes no contribution to Eq. (18). Thus, it is important to accurately model the behavior of the eigenmode for $q_x\lesssim q_c$, but not for the very small scale limit of $q_x\gg q_c$. Further, since Eq. (17) does not possess any singularities, ϕ as well as its derivatives must be continuous. More simply put, there is no MHD exterior with which to match, so no discontinuity in ψ' occurs. Thus, we are able to separate the solutions into even and odd parity modes, given by $\partial\phi/\partial q_x|_{q_x=0}=0$ for the even parity mode, and $\phi(q_x=0)=0$ for the odd parity mode. The trial functions for the even and odd parity mode can then be written as

$$\phi_{\mathrm{even}}=\sqrt{q_x}I_{-1/4}\left(\frac{x_T^2q_x^2}{2}\right),\quad |q_x|<q_c$$

$$\phi_{\mathrm{even}}=\{C_1^e\mathrm{Ai}(-\alpha(q_x-q_c))-C_2^e\mathrm{Bi}(-\alpha(q_x-q_c))\}e^{-\alpha^2(q_x-q_c)^2},\quad |q_x|>q_c \tag{24}$$

$$\phi_{\mathrm{odd}}=\sqrt{q_x}I_{1/4}\left(\frac{x_T^2q_x^2}{2}\right),\quad |q_x|<q_c$$

$$\phi_{\mathrm{odd}}=\{C_1^o\mathrm{Ai}(-\alpha(q_x-q_c))-C_2^o\mathrm{Bi}(-\alpha(q_x-q_c))\}e^{-\alpha^2(q_x-q_c)^2},\quad |q_x|>q_c$$

where the coefficients C_1^e, C_2^e, C_1^o, and C_2^o are set by matching to the solution for $|q_x|<q_c$, and the exponential has been introduced to ensure convergence of the integrals in the quadratic form. A plot of the general structure of the trial functions is given in Fig. 5. Note that these functions converge much more rapidly for large q_x than the asymptotic solutions derived above. However, in both cases the contribution to the variational form above rapidly vanishes, either by the numerator identically canceling, or by each integral separately vanishing.

Upon performing the integrals within Eq. (18), the scaling form of the growth rate for both the even and odd modes is given by

$$\gamma_q\sim\frac{|\nu_{xx}|^{2/3}(v_Aq_y)^{2/3}}{\eta_c^{1/3}}\frac{1}{L_s^{2/3}}\sim\mathrm{Pr}^{2/3}\tau_\eta^{-1/3}\tau_A^{-2/3}, \tag{25}$$

where Pr is the Prandtl number, defined here as $\mathrm{Pr}=|\nu_{xx}|/\eta_c$, and τ_η and τ_A are the resistive time and Alfvén time, respectively. This expression can be rewritten in the form $\gamma_q\sim|\nu_{xx}|/\Delta_q^2$, where Δ_q gives the width of the vortex mode and is defined as

$$\Delta_q=x_\nu=(\eta_c|\nu_{xx}|)^{1/6}\left(\frac{L_s}{q_yv_A}\right)^{1/3}. \tag{26}$$

At this point it is necessary to check the validity of the electrostatic approximation. Writing Eq. (14) as:

$$\eta_c\frac{\partial^2\psi^<}{\partial x^2}=\gamma_q\psi^<-iq_yv_A\frac{x}{L_s}\phi^<, \tag{27}$$

it is clear that in order for the electrostatic approximation to be valid $\eta_c/x_\nu^2>\gamma_q$. This can be rewritten as $|\nu_{xx}|/\eta_c=P<1$, which corresponds to $D_{\mathrm{GB}}/\eta_c<1$. Also, note that this criteria explains the divergence of γ_q with $\eta_C\to0$, since as η_c goes to zero, the turbulent viscosity must also vanish in order for the Prandtl number to remain finite.

It is useful at this point to contrast the vortices generated by inverse cascade of energy in 2D hydrodynamic turbulence

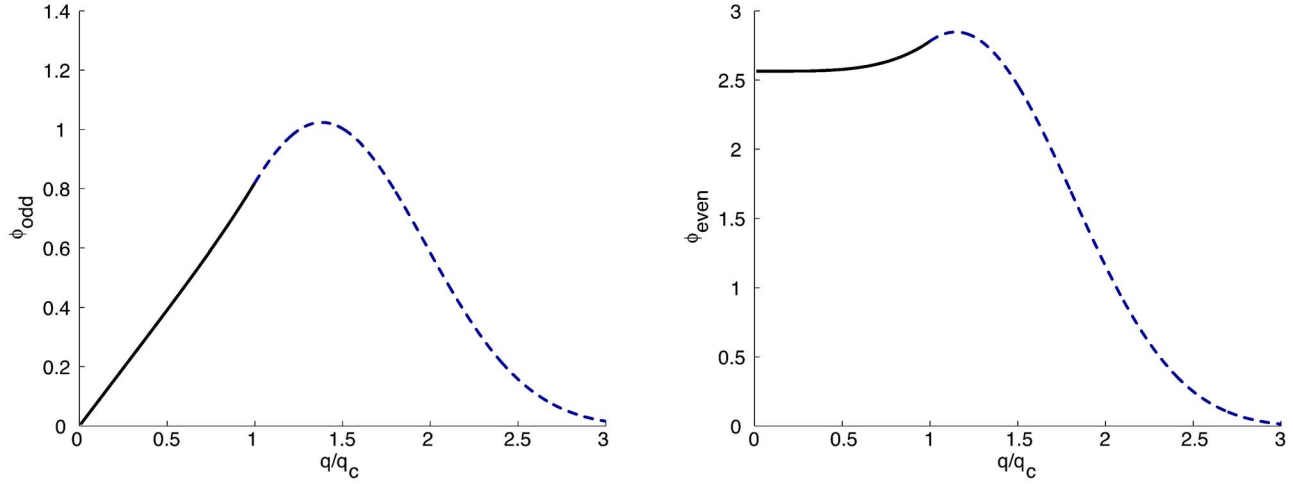

FIG. 5. Plots of even and odd trial functions. The solid line indicates the solution for $q<q_c$, whereas the broken line indicates the solution for $q>q_c$.

with those generated in a strongly magnetized plasma by drift wave turbulence. In both systems enstrophy and kinetic energy are inviscid constants of the motion. This leads to the existence of dual cascade ranges for energy and enstrophy. 2D hydrodynamic turbulent systems forced on a scale smaller than the system size generate large scale vortices (of the order of the system size, see, e.g., Ref. 31 and references there in) due to an inverse cascade of energy. However, an important *difference* between the case of drift wave turbulence and "fluid in a box" is that as both systems exhibit spectral condensation of energy on the large scales, 2D hydrodynamic turbulence has a tendency to form vortices on the order of the system size (i.e., isotropic cells). However, for a magnetized plasma with $q=q(r)$, the energetics of field line bending implies that the vortices will be *strongly anisotropic cells of narrow radial extent*.

B. Reconnecting mode

In the analysis mentioned previously, we discussed an electrostatic vortex mode pumped by the inverse cascade via the negative viscosity. However, a negative viscosity will also have a strong impact on the linear dynamics of the reconnecting mode, i.e., the counterpart, for this study, of the traditional tearing mode. Integrating Eq. (14) across the resistive layer, and writing Eq. (15) in dimensionless units gives

$$0=\mathrm{sgn}(\nu_{xx})\frac{\partial^4\Phi}{\partial\sigma^4}-\frac{1}{\alpha}\frac{\partial^2\Phi}{\partial\sigma^2}+\sigma(1+\sigma\Phi), \tag{28}$$

$$\Delta'=-\frac{i\omega_q}{\eta_c}x_\nu\int d\sigma(1+\sigma\Phi), \tag{29}$$

where $\Delta'=(\psi'(0^+)-\psi'(0^-))/\psi_0$, $\alpha=i|\nu_{xx}|/\omega_q x_\nu^2$, $\sigma=x/x_\nu$, $\Phi=(q_y v_A/\omega_q)(x_\nu/L_s)(\phi^</\psi_0^<)$, $x_\nu=(\eta_c|\nu_{xx}|)^{1/6}(L_s/q_y v_A)^{1/3}$. In the limit $\xi^2/\alpha\sim|(x_\nu^2/\nu_{xx})\omega_q|<1$ (i.e., the viscous dominated regime), the inertial term (second term on the right-hand side) is negligible, and Eq. (28) reduces to

$$0=\mathrm{sgn}(\nu_{xx})\frac{\partial^4\Phi}{\partial\sigma^4}+\sigma(1+\sigma\Phi). \tag{30}$$

In order to lower the order of the previous equations, it will be convenient to introduce the Fourier transform defined by $\Phi(q_x)=\int_{-\infty}^{\infty}d\sigma e^{-iq_x\sigma}\Phi(\sigma)$. Here the integration is over the solutions within the singular layer. Eqs. (29) and (30) then become[28]

$$\frac{d^2\Phi(q_x)}{dq_x^2}-\mathrm{sgn}(\nu_{xx})q_x^4\Phi(q_x)=2\pi i\frac{d}{dq_x}\delta(q_x), \tag{31}$$

$$\Delta'=-\frac{i\omega_q}{\eta_c}x_\nu\left(2\pi\delta(q_x)+i\left.\frac{d\Phi(q_x)}{dq_x}\right|_{q_x=0}\right). \tag{32}$$

The solution of Eq. (31) is given by

$$\Phi(q_x)=i\pi\,\mathrm{sgn}(q_x)\frac{\Phi_{\mathrm{hom}}(|q_x|)}{\Phi_{\mathrm{hom}}(0)}. \tag{33}$$

Substituting Eq. (33) into Eq. (32) gives the eigenvalue relation in terms of the homogeneous solution

$$\Delta'=-i\pi\frac{\omega_q}{\eta_c}x_\nu\frac{1}{\Phi_{\mathrm{hom}}(0)}\left.\frac{d\Phi_{\mathrm{hom}}}{dq_x}\right|_{q_x=0}. \tag{34}$$

Before discussing the effect of a negative viscosity on the reconnecting mode, it is useful to briefly review the *positive viscosity* case ($k_x(\partial N_k^0/\partial k_x)>0$). Following Ref. 28 closely, the homogeneous solution of Eq. (31) is given by

$$\Phi_{\mathrm{hom}}(q_x)=A\sqrt{q_x}I_{1/6}\left(\frac{q_x^3}{3}\right)+B\sqrt{q_x}K_{1/6}\left(\frac{q_x^3}{3}\right), \tag{35}$$

where A and B are arbitrary constants, and I and K represent modified Bessel functions. Since the I solution diverges exponentially for large q_x, we retain only the K piece. Expanding Eq. (35) (with A set to zero), yields to first order

$$\Phi(q_x) \approx B\left(\pi\frac{6^{1/6}}{\Gamma\left(\frac{5}{6}\right)} - \frac{1}{6^{1/6}}\frac{\pi}{\Gamma\left(\frac{7}{6}\right)}q_x\right). \tag{36}$$

After inserting Eq. (36) into Eq. (34), the dispersion relation obtained is

$$\gamma_q = \frac{6^{1/3}}{\pi}\frac{\Gamma\left(\frac{7}{6}\right)}{\Gamma\left(\frac{5}{6}\right)}\frac{\eta_c^{5/6}}{\nu_{xx}^{1/6}}\left(\frac{q_y v_A}{L_s}\right)^{1/3}\Delta'$$

$$\approx 0.48\frac{\Gamma\left(\frac{7}{6}\right)}{\Gamma\left(\frac{5}{6}\right)}\frac{\eta_c^{5/6}}{\nu_{xx}^{1/6}}\left(\frac{q_y v_A}{L_s}\right)^{1/3}\Delta' \sim P^{-1/6}\tau_\eta^{-2/3}\tau_A^{-1/3}, \tag{37}$$

which is identical to the expressions derived in Refs. 28 and 29. Note that the limit $\nu_{xx}\to 0$ is unimportant, as the result of Eq. (37) is valid only for the viscosity dominated regime. Further, the growth rate can be seen to be (weakly) inversely proportional to ν_{xx}. Physically this can be understood as viscous damping reducing the strength of the fluid eddies driven by the linear $\mathbf{J}\times\mathbf{B}$ force.

Now, we consider the more subtle case of a negative viscosity ($k_x\partial N_k^0/\partial k_x<0$). It is useful to first consider the form of Eq. (30) in real space, i.e.,

$$0 = -\frac{\partial^4\Phi}{\partial\sigma^4} + \sigma(1+\sigma\Phi). \tag{38}$$

Note that the effect of changing the sign of the fourth order derivative is to introduce solutions that oscillate rapidly, which we are unable to match to the second order exterior solution. It is useful at this point to construct an eikonal formulation of the solution of Eq. (38), for large σ. We proceed by considering solutions of the form $\Phi(\sigma)=f(\sigma)e^{i\psi(\sigma)} - 1/\sigma$, where $f(\sigma)$ corresponds to a slowly varying amplitude, and $\psi(\sigma)$ corresponds to a rapidly varying phase. Eq. (38) then becomes:

$$0 = -\frac{d^4}{d\sigma^4}\left(fe^{i\psi} - \frac{1}{\sigma}\right) + \sigma\left(1+\sigma\left(fe^{i\psi} - \frac{1}{\sigma}\right)\right). \tag{39}$$

Only solutions which die off slower than $1/\sigma$ are relevant for large σ. This allows us to drop the fourth derivative of $1/\sigma$. Taking derivatives, and separating the real and imaginary parts, gives:

$$0 = -f'''' + 6f''(\psi')^2 + 9f'\psi'\psi'' + 4f\psi'\psi''' + 3f(\psi'')^2 - f(\psi')^4 + \sigma^2 f, \tag{40}$$

$$0 = -4f'''\psi' - 6f''\psi'' - 4f'\psi''' + 4f'(\psi')^3 - f\psi'''' + 6f(\psi')^2\psi'', \tag{41}$$

where f' and ψ' denote derivatives with respect to σ. Derivatives of the amplitude are by assumption slow in comparison with derivatives with respect to the phase, thus to lowest order:

$$0 = -f(\psi')^4 + \sigma^2 f, \tag{42}$$

$$0 = 4f'(\psi')^3 + 6f(\psi')^2\psi''. \tag{43}$$

After canceling f in Eq. (42), solving for ψ, then plugging into Eq. (43) an expression valid for large σ can be derived, yielding:

$$\Phi(\sigma) = \mathrm{sgn}(\sigma)\frac{D}{|\sigma|^{3/4}}\exp\left(i\frac{2}{3}|\sigma|^{3/2} + i\phi_D\right) + \mathrm{sgn}(\sigma)\frac{E}{|\sigma|^{3/4}}\exp\left(-i\frac{2}{3}|\sigma|^{3/2} + i\phi_E\right) - \frac{1}{\sigma}. \tag{44}$$

The oscillatory terms in this expression result from balancing the fourth order viscous term, against $\sigma^2\Phi$, the linear $\mathbf{J}\times\mathbf{B}$ force. It follows that the $\gamma_q\psi^<$ term plays no role in determining the structure of the oscillations. Thus, the general form of this solution can be understood as a consequence of coupling the *electrostatic vortex mode to the low-m tearing mode, which connects to the ideal MHD exterior*. From this expression we note that the oscillations die off more slowly than the residual tearing mode term. Hence, *unless some other mechanism damps the oscillations, it is not possible to match the oscillatory solutions to the exterior solution*. In Fourier space, this can be understood by considering the homogeneous solution of Eq. (31), which is

$$\Phi_{\mathrm{hom}}(q_x) = A\sqrt{q_x}J_{1/6}\left(\frac{q_x^3}{3}\right) + B\sqrt{q_x}Y_{1/6}\left(\frac{q_x^3}{3}\right). \tag{45}$$

Two observations concerning this equation are possible. First, upon Fourier transforming Eq. (45), the solutions in real space can be seen to undergo oscillations which are 90° out of phase with one another (Fig. 6). Thus, fixing the ratio of the amplitudes A/B is equivalent to setting the phase of the oscillations. Second, since both of these solutions converge for $q_x\to\infty$, neither solution can be dropped. These considerations leave us with an undetermined constant A/B in the eigenvalue relation, which can be written as

$$\Delta' = -i\frac{\pi}{2}\frac{1}{6^{1/6}}\frac{\Gamma\left(\frac{5}{6}\right)}{\Gamma\left(\frac{7}{6}\right)}\frac{\omega_q}{\eta_c}x_\nu\left(\frac{3^{1/3}}{2^{1/6}} + \frac{1}{6^{1/6}}\frac{A}{B}\right). \tag{46}$$

From this expression it is clear that another boundary condition is needed in order to specify A/B in the dispersion relation, Eq. (46). This extra boundary condition corresponds to setting the phase of the oscillations of the solution. Thus, the boundary condition *cannot* be determined from the solution in the exterior region alone. To control the oscillations in the solution produced by the negative viscosity, and to allow matching to the ideal MHD exterior, it is necessary to impose a condition on the wave energy flux. The only physically consistent condition is that of outgoing waves. Outgoing waves are absorbed at resonance points away from $x=0$. The outgoing wave boundary condition is justified by noting that free energy (from either tearing or negative viscosity) is released only near the resonant surface at $x=0$, whereas for $x\to\infty$ the system is ideal MHD so the frozen-in law applies. Hence, no energy release is possible in the exterior ($x\to\infty$) region. Thus, there is no energy to carry by incoming waves.

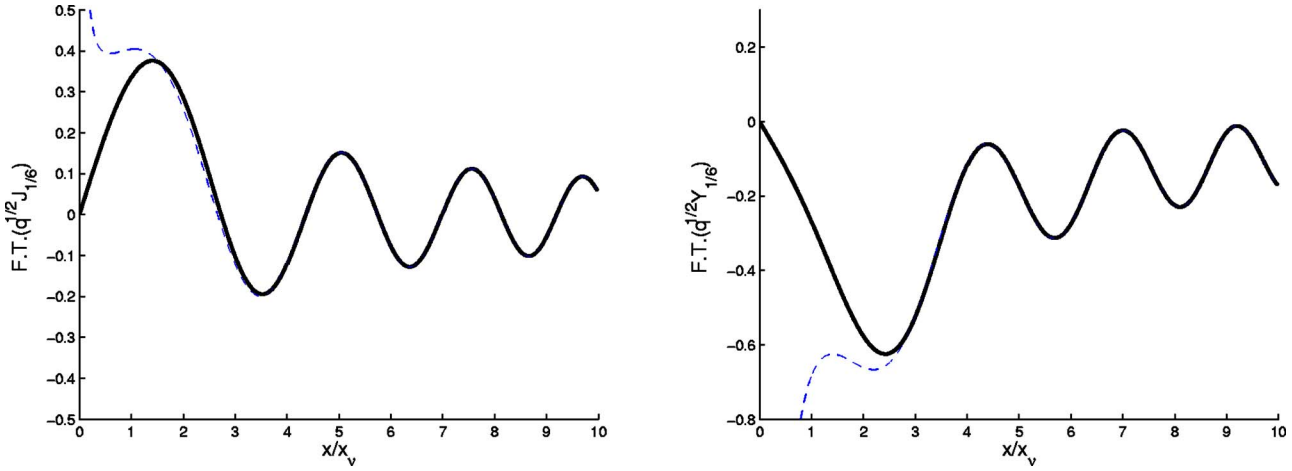

FIG. 6. Plots of eikonal solutions versus exact solution. The solid lines correspond to the exact solutions, whereas the broken lines correspond to the eikonal solutions.

We see then, that outgoing wave boundary conditions are the only physically plausible choice. Note that a real frequency appears (self-consistently) as well, so wave absorption is in fact possible. Finally, we note that previous studies of (ω^*) modified tearing modes have invoked outgoing wave boundary conditions for similar reasons.[32] Like other familiar cases of outgoing wave boundary conditions, the damping does not appear *explicitly* in the theory, as outgoing wave boundary conditions *tacitly presume a sink* for the outgoing wave.

As shown in Appendix A, this outgoing wave energy condition implies that A/B is pure imaginary, so the dispersion relation takes the form

$$\gamma_q \sim \frac{\eta_c}{x_\nu}\Delta' \sim \frac{\eta_c^{5/6}}{|\nu_{xx}|^{1/6}}\left(\frac{q_y v_A}{L_s}\right)^{1/3}\Delta', \tag{47}$$

$$\mathrm{Re}(\omega_q) \sim \frac{\eta_c^{5/6}}{|\nu_{xx}|^{1/6}}\left(\frac{q_y v_A}{L_s}\right)^{1/3}\Delta', \tag{48}$$

where Δ' is purely real. Note that here the growth rate and frequency have the same scaling. This is primarily a consequence of neglecting the electron pressure gradient and other "two fluid" and kinetic effects. Including the electron and ion diamagnetic drift into the mean field equations yields a dispersion relation of the form $\gamma_\nu^6/(1+ic_1)^6 \sim -(\omega_q-\omega_e^*)^5(\omega_q-\omega_i^*)$, where c_1 is a number of order unity set by matching to the eikonal solution. In the limit $\gamma_\nu \ll \omega_e^*$, which is relevant for drift tearing modes, the real frequency is given approximately by $\mathrm{Re}(\omega_q) \approx \omega_e^*$.

IV. CONCLUSIONS AND DISCUSSION

In this article, we have explored a minimal self-consistent model of the multiscale interaction of a tearing mode with ambient, electrostatic drift wave turbulence. The principal results of this paper are as follows.

(1) Its self-consistent formulation in terms of Reynolds stress effects of small scales (drift waves) upon large scales (tearing mode), along with the backreaction of large scale straining and shearing flows on small scale turbulence. Here, the multiscale interaction is described by nonlinear modulation of the drift wave intensity field by the tearing mode flows.
(2) The identification of the *negative* turbulent viscosity as the principal effect of electrostatic drift wave turbulence on a simple, low-m tearing mode. Thus, the low-q resonance by the turbulent inverse cascade.
(3) the identification of low-m, resonant electrostatic modes which are nonlinearly driven by the inverse cascade (via negative viscosity) and damped by resistivity modified field line bending. These anisotropic "vortex modes" have growth rate $\gamma_q \sim (|\nu_{xx}|^{2/3}(v_A q_y)^{2/3}/\eta_c^{1/3})(1/L_s^{2/3})$ and radial extent $\Delta_q = (\eta_c|\nu_{xx}|)^{1/6}(L_s/q_y v_A)^{1/3}$, and can couple to the tearing mode.
(4) The calculation of the growth rate of a "reconnecting mode" (with $\Delta' > 0$), which couples to an ideal MHD exterior. This is the analog of the familiar tearing mode, but with negative viscosity providing the coupling to background turbulence. Moreover, for typical "mixing length level" turbulence amplitudes, inertia is negligible, even in the *linear growth phase*. The reconnecting mode has a growth rate $\gamma_q \sim (\eta_c^{5/6}/|\nu_{xx}|^{1/6})((q_y v_A/L_s))^{1/3}\Delta'$ and layer width $\Delta_q = (\eta_c|\nu_{xx}|)^{1/6}(L_s/q_y v_A)^{1/3}$. Outgoing wave boundary conditions must be imposed to match the inner layer to the MHD exterior.

In addition to presenting the specific results enumerated above, we take this opportunity to briefly discuss some broader implications of this work. The classical Rutherford regime[33] corresponds to a filamented "near equilibrium" state, which evolves slowly and self-similarly in time. Consistent with self-similarity, the magnetic island width grows with a power of time (i.e., proportional to t), as opposed to exponentially in time, as in the linear phase. It is interesting to note that in the presence of turbulence at the "typical," Gyro-Bohm level, the negative viscosity term dominates inertia, *even in the linear phase*. However, it is by no means clear that the negative viscosity is a-priori negligible in the Rutherford phase. Further, since the Rutherford phase is one of slow evolution, keeping finite flow excitation by negative

viscosity compels us to also retain *damping* of the low-m flows.

As mentioned in the previous paragraph, it is important to take note of the conceptual distinction between the classical Rutherford state and the nonlinear evolution of the reconnecting mode discussed here. In the classic Rutherford calculation, the balance is first plus third order $\mathbf{J}\times\mathbf{B}$ forces versus inertia, leading to $\mathbf{B}\cdot\nabla J=(d/dt)\nabla_\perp^2\phi$. For island width exceeding tearing layer width (i.e., $w_I>x_T$), $(\mathbf{B}\cdot\nabla J)^{(3)}>(d/dt)\nabla_\perp^2\phi$, so this relation simplifies to $\mathbf{B}\cdot\nabla J=0$. Thus, $J=J(\psi)$ can be inserted into Ohms Law, yielding a differential equation for the evolution of the island width. Here, for finite island size, the balance becomes

$$\mathbf{B}\cdot\nabla J=-\frac{\partial^2}{\partial x^2}\left(\int d\vec{k}\frac{k_x k_y}{(1+\rho_s^2 k_\perp^2)^2}\delta N_k(x,t)\right)+\gamma[\nabla^2\phi]. \tag{49}$$

Here the second term on the right-hand side refers to the modulation of the turbulent vorticity transport (i.e., Reynolds stress) by the island and $\gamma[\nabla^2\phi]$ refers to the neoclassical flow damping,[34,35] which may need to account for island-induced toroidal symmetry breaking.

Thus, the $\mathbf{J}\times\mathbf{B}$ force equals the imbalance between the flow drive induced by modulation of the Reynolds stress and the flow damping. Both of the latter two depend upon island size. Note that in the *complete absence of an island*, Eq. (49) reduces to the marginality condition for the modulation stability of a low-m vortex or zonal flow (for $m=0$). Similarly, neglecting *both* turbulence modulation and flow damping recovers "classical Rutherford," namely $\mathbf{B}\cdot\nabla J=0$. Thus, the structure outlined in Eq. (49) recovers both of the requisite limiting cases. It follows that the island current is the sum of a Δ'-driven contribution (associated with the homogeneous solution $J(\psi)$) and a contribution due to the *competition* between flow generation and damping. Note that both $\delta N(\mathbf{k},x,t)$ and γ in Eq. (49) must be computed as a function of the island width w_I, and will depend nonlinearly upon it. Note also that, as mentioned after Eq. (49), retaining both $\partial N_k^0/\partial x$ and $\partial N_k^0/\partial\mathbf{k}$ contributions to δN_k guarantees turbulence driven contributions to the current J that are *both* real and imaginary. Further discussion of the finite island calculation is beyond the scope of this paper, and will be addressed in a future publication.

As discussed in Sec. III, the theory of finite size magnetic islands must be extended to encompass excitation of island flows by turbulence modulation and the damping of flows due to breaking of axisymmetry. Any imbalance between these two effects will produce a current which in turn affects island size. Second, in reference to the finite size island case, the reader should keep in mind that the turbulence intensity profile ($\sim N(\mathbf{k},x,t)$) is *not static*. In particular, flattening of $\nabla_\mathbf{x}N$ within an island will likely steepen $\nabla_x N$ in adjacent regions, which results in either a "backwash" of turbulence spreading or the possible formation of a transport barrier, since steep $\nabla_x N$ in turn implies enhanced flow and flow shear drive via Reynolds stress.[36,37] Clearly, some sort of bifurcation condition delimits the boundary between these two very different "basin's of attraction" for the system state. Significant further work is required to elucidate this transition.

A second speculation engendered by this work is concerned with the possible relation between low-q resonances and observed profile corrugations and transport barriers.[38] The question of the role of low-q surfaces in confinement has a long history.[39–43] Low-q surfaces have in the past been associated with microtearing modes, magnetic islands of unexplained origin, etc., all with the aim of providing a physical basis for the notion of profile consistency. Previous work[44] has also suggested that spikes or humps in the fluctuation intensity profile may sit at low-q resonances, and that these localized intensity gradients may drive sheared poloidal flow via the Reynolds stress. These flows are "mean" flows, but sharply localized in radius. Very recently work has proposed that, profile corrugations at low-q resonances are related to the formation of localized zonal flows. Here, we would like to add the suggestion that since low-q resonances are natural locations for the "vortex mode" we have discussed that, too, may enter the already complicated story of resonant q. Note also that the vortex mode is intrinsically quite narrow, in contrast to the zonal flow, which can be quite broad. Thus, the vortex mode is an interesting candidate for the observed corrugations.

We also again emphasize here that this model is indeed a "minimalist" "toy" model, which omits many detailed effects relevant to NTM evolution in tokamaks. These include, but certainly are not limited to the effects of toroidicity and bootstrap current drive, the effects of turbulent heat transport on island evolution, neoclassical modifications of the polarization drift, island-induced modifications of the density, temperature and turbulence intensity profiles, incoherent emission from turbulence, spreading of turbulence from adjacent regimes into the island, etc. Indeed, the list is endless. Many years of interesting research will be necessary to resolve these and the other interesting questions pertinent to the theory of multiscale interaction of turbulence with MHD.

ACKNOWLEDGMENTS

The authors gratefully acknowledge many useful and fascinating discussions especially with Susanna Cappello and Dominique Escande who strongly stimulated our interest in this problem. They also thank A. Smolyakov, M. Yagi, S-I Itoh, K. Itoh, T.S. Hahm, X. Garbet, J. Connor, H. Wilson, and Ö. D. Gürcan for helpful discussions. Thanks also go to M. Austin and K. Burrell for sharing unpublished information concerning the effect of low-q resonances on confinement. Also, they would like to thank Ö. D. Gürcan for a careful reading of the manuscript. Many of these interactions were fostered by the Festival de Théorie, at Aix-en-Provence in 2003, 2005. One of the authors (P.D.) also acknowledges the hospitality of Kyushu University, where part of this work was performed.

This research was supported by Department of Energy, under Contract No. DE-FG02-04ER54738.

APPENDIX A: OUTGOING WAVE ENERGY BOUNDARY CONDITIONS

In order to calculate the ratio A/B in Eq. (46), it is necessary to match our exact solution Eq. (45) to the outgoing piece of the eikonal solution. The fluctuating piece of Eq. (44) can be rewritten as

$$\tilde{\Phi}(\sigma) = \mathrm{sgn}(\sigma)\frac{D}{|\sigma|^{3/4}}e^{ik_x|x|+i\phi_D} + \mathrm{sgn}(\sigma)\frac{E}{|\sigma|^{3/4}}e^{-ik_x|x|+i\phi_E}, \tag{A1}$$

where k_x is defined as $k_x=(2/3)\sqrt{|x|}/x_\nu^{3/2}$. k_x can be related to the frequency through the dispersion relation $Re(\omega_q) \sim (\eta_c\Delta')/x_\nu$, which yields $k_x \sim \sqrt{|x|}\omega_q^{3/2}/(\eta_c\Delta')^{3/2}$. Thus, the sign of v_{gr} can be determined from $v_{\mathrm{gr}}^{-1}=\partial k_x/\partial\omega_q$. Applying the outgoing wave energy boundary condition then gives (for large values of x, i.e., $x \gg x_\nu$)

$$\tilde{\Phi}(x) = \mathrm{sgn}(x)\frac{D}{|\sigma|^{3/4}}e^{ik_x|x|+i\phi_D}. \tag{A2}$$

We are now interested in matching the exact solution to the eikonal solution, in order to determine the ratio A/B. The exact solution in Fourier space can be written as

$$\Phi(q_x) = -i\frac{\pi^2}{\Gamma(1/6)}\frac{1}{6^{1/6}}\mathrm{sgn}(q_x)\left\{\frac{A}{B}\sqrt{|q_x|}J_{1/6}\left(\frac{|q_x|^3}{3}\right) + \sqrt{|q_x|}Y_{1/6}\left(\frac{|q_x|^3}{3}\right)\right\}. \tag{A3}$$

This solution can be rewritten in real space as

$$\begin{aligned}\frac{1}{2\pi}\int dq_x e^{iq_x\sigma}\,\mathrm{sgn}(q_x)\sqrt{|q_x|}J_{1/6}\left(\frac{|q_x|^3}{3}\right) &= i6^{(4/3)}\Gamma(-2/3)\Gamma(7/6)\sigma_0F_3\left(\frac{2}{3},\frac{5}{6},\frac{7}{6};\frac{\sigma^6}{1296}\right)\\ &+ i\frac{1}{18\sqrt{2}\pi}\frac{\Gamma(-1/3)}{\Gamma(7/6)}\sigma^3{}_0F_3\left(\frac{7}{6},\frac{4}{3},\frac{3}{2};\frac{\sigma^6}{1296}\right),\end{aligned} \tag{A4}$$

and

$$\begin{aligned}\frac{1}{2\pi}\int dq_x e^{iq_x\sigma}\,\mathrm{sgn}(q_x)\sqrt{|q_x|}Y_{1/6}\left(\frac{|q_x|^3}{3}\right) &= -i\frac{1}{2(6)^{1/6}}\frac{1}{\pi^{3/2}}\Gamma(1/3)\sigma_0F_3\left(\frac{2}{3},\frac{5}{6},\frac{7}{6};\frac{\sigma^6}{1296}\right)\\ &+ i\frac{\sqrt{6}}{30\pi^2}\Gamma(-1/3)\Gamma(-11/6)\sigma^3{}_0F_3\left(\frac{7}{6},\frac{4}{3},\frac{3}{2};\frac{\sigma^6}{1296}\right)\\ &+ i\frac{6^{1/6}}{120\pi^2}\sigma^5{}_1F_4\left(1;\frac{4}{3},\frac{3}{2},\frac{5}{3},\frac{11}{6};\frac{\sigma^5}{1296}\right),\end{aligned} \tag{A5}$$

where ${}_pF_q$ is a generalized hypergeometric function. Matching Eq. (A3) to Eq. (A2), with the use of Eqs. (A4) and (A5), leads to $A/B=i$. A plot comparing the eikonal solutions to the exact solutions is given in Fig. 6.

APPENDIX B: WAVE KINETIC EQUATION FOR ITG TURBULENCE IN SHEARED MAGNETIC FIELD

In the main text we considered an absolutely minimal model of the background microturbulence in order to illuminate a number of the salient features of the tearing mode-drift wave interaction. Here, we are also interested in introducing a somewhat more sophisticated model of the ambient microturbulence by including the impact of magnetic shear on the linear mode structure. As will be seen below, when magnetic shear is added to the system, the extent of the radial localization, and thus the degree of anisotropy, all affect the linear dynamics.

We begin by considering a set of fluid equations which model ITG turbulence in the presence of a sheared magnetic field. The linear eigenmode and dispersion relation, similar to that derived in Ref. 45, but here we include a curvature term relevant for the RFP, are given by:

$$\begin{aligned}&\phi_k(x) \sim e^{-(i/2)\mu_k x^2},\\ &\mu_k = -\frac{1}{L_s}\frac{|k_y|}{|\omega_{k_y}|^2}(\omega_{k_y}-i\gamma_{k_y})\left(1-\frac{2}{R}\frac{k_y}{\omega_{k_y}}\frac{\Gamma}{\tau}\right)^{1/2}\\ &0 = (1+k_y^2)\omega_{k_y}^2 + v_e^*k_y\left[\frac{i}{|L_s|}\frac{1}{v_e^*}\,\mathrm{sign}(k_y)\left(1-\frac{2}{R}\frac{k_y}{\omega_{k_y}}\frac{\Gamma}{\tau}\right)^{1/2} + k_y^2\kappa + 2\frac{L_n}{R}-1\right]\omega_{k_y} + \frac{2}{R}\kappa k_y^2v_e^*\\ &\quad + \frac{i}{|L_s|}\kappa\,\mathrm{sign}(k_y)k_y^2v_e^*\left(1-\frac{2}{R}\frac{k_y}{\omega_{k_y}}\frac{\Gamma}{\tau}\right)^{1/2}.\end{aligned} \tag{B1}$$

$$(\phi^>(\vec{x},t),P^>(\vec{x},t),V^>(\vec{x},t)) = \int d^2k(\phi_k^>(x,t),P_k^>(x,t),V_k^>(x,t))e^{iky+ik_zz}, \tag{B2}$$

where k_y has been written as k. Thus, the vorticity equation[45] will now take the form

$$\begin{aligned}0 = \partial_t(1-\partial_{xx}+k^2)\phi_k^>(x,t) &+ iV_e^*k\left(1-2\frac{L_n}{R}+\kappa(\partial_{xx}-k^2)\right)\\ &\times\phi_k^>(x,t) - \frac{2i}{R}kP_k^>(x,t) + ik_zV_k^>(x,t)\\ &- i\sum_{k=k_1+k_2}k_1\phi_{k_1}^<(x,t)(1-\partial_{xx}+k_2^2)\partial_x\phi_{k_2}^>(x,t)\\ &+ i\sum_{k=k_1+k_2}k_2\partial_x\phi_{k_1}^<(x,t)(1-\partial_{xx}+k_2^2)\phi_{k_2}^>(x,t).\end{aligned} \tag{B3}$$

Here the summations are short hand notation for integrations, i.e., $\Sigma_{k=p+q}\rightarrow\int dpdq\,\delta(-k+p+q)$. It is now useful to separate

the time dependence of the small scale fields into a slowly varying amplitude (resulting from the modulations of the large scale mean fields), and a rapidly varying piece, so that:

$$(\phi_k^>(x,t),P_k^>(x,t),V_k^>(x,t)) \rightarrow (a_k(t)e^{-i\omega_k t}\phi_k^>(x),b_k(t)e^{-i\omega_k t}P_k^>(x),c_k(t)e^{-i\omega_k t}V_k^>(x)), \tag{B5}$$

where $\phi_k^>(x)$ is the linear eigenmode, and x is defined as the distance from the $r_{m,n}$ resonant surface ($k_1=m_1/r$ and $k_{1z}=n_1/R$). We can now define a Wigner function as $I_k(y,t)=\int dp e^{ipy}\langle a_{k+p}(t)e^{-i\omega_{k+p}t}a_{-k}(t)e^{-i\omega_{-k}t}\rangle$. We choose the normalization $\int dx\phi_k^>(x)\phi_{-k}^>(x)=1$ for the radial eigenmodes, where $\mu_{-k}^{(r)}=-\mu_k^{(r)}$ and $\mu_{-k}^{(i)}=\mu_k^{(i)}$. An equation describing the evolution of the intensity of the drift wave turbulence can be derived by multiplying Eq. (B4) (with $k\rightarrow -k$) by $\phi_{k'}^>(x,t)$, and adding the same equation with $-k\leftrightarrow k'$. Setting $k'=k+p$, where p corresponds to the wave number of the large scales, and neglecting the cross terms for reasons of simplicity, gives:

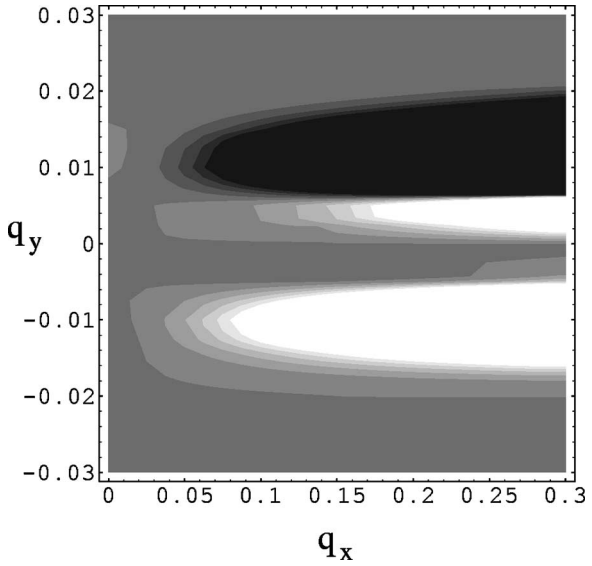

FIG. 7. Plot of $C(\mathbf{q})$ as a function of q_y and q_x.

$$\begin{aligned}
&\phi_{-k}^>(x)\phi_{k+p}^>(x)\left(\frac{\partial}{\partial t}+i(\omega_{-k}+\omega_{k+p})\right)(a_{-k}(t)e^{-i\omega_{-k}t}a_{k+p}(t)e^{-i\omega_{k+p}t}) \\
&=i\sum_{-k=k_1+k_2}a_{k+q}\exp(-i\omega_{k+p}t)a_{k_2}\exp(-i\omega_{k_2}t)k_1\phi_{k+p}^>(x)(1-\partial_{xx}+k_2^2)\partial_x\phi_{k_2}^>(x)\phi_{k_1}^<(x,t)-i\sum_{-k=k_1+k_2}a_{k+q}\exp(-i\omega_{k+p}t)a_{k_2} \\
&\times\exp(-i\omega_{k_2}t)k_2\phi_{k+p}^>(x)(1-\partial_{xx}+k_2^2)\phi_{k_2}^>(x)\partial_x\phi_{k_1}^<(x,t)-i\sum_{k+p=k_1+k_2}a_{-k}\exp(-i\omega_{-k}t)a_{k_2} \\
&\times\exp(-i\omega_{k_2}t)k_1\phi_{-k}^>(x)(1-\partial_{xx}+k_2^2)\partial_x\phi_{k_2}^>(x)\phi_{k_1}^<(x,t)+i\sum_{k+p=k_1+k_2}a_{-k}\exp(-i\omega_{-k}t)a_{k_2} \\
&\times\exp(-i\omega_{k_2}t)k_2\phi_{-k}^>(x)(1-\partial_{xx}+k_2^2)\phi_{k_2}^>(x)\partial_x\phi_{k_1}^<(x,t),
\end{aligned} \tag{B6}$$

$$\phi_{-k}^>(x)\phi_{k+p}^>(x)\left(\frac{\partial}{\partial t}+i(\omega_{-k}+\omega_{k+p})\right)\times(a_{-k}(t)e^{-i\omega_{-k}t}a_{k+p}(t)e^{-i\omega_{k+p}t})=S_1+S_2+S_3+S_4.$$

Here ω_k includes the real frequency and growth rate of the linear mode. In order to simplify the notation we define $\tilde{a}_k(t)=a_k(t)e^{-i\omega_k t}$. Expanding the linear piece in the ratio $p/k\ll 1$, averaging over the fast scales, integrating across the distribution of resonant surfaces, applying the operator $\int dp e^{ipy}$, and using the normalization condition gives the evolution equation for I_k which is:

$$\left(\frac{\partial}{\partial t}+v_{gr}\frac{\partial}{\partial y}+\gamma_k\right)I_k=\int dp e^{ipy}\int dx\langle S_1+S_2+S_3+S_4\rangle, \tag{B7}$$

where γ_k includes both the linear growth rate of the ITG mode, as well as the shear damping piece. In order to evaluate the nonlinear terms it is useful to inverse Fourier transform the ensemble averaged terms,[22] i.e., for S_1

$$\langle\tilde{a}_{k+p}(t)\tilde{a}_{-k+k_1}(t)\rangle=\langle\tilde{a}_{(-k+k_1)+(p-k_1)}(t)\tilde{a}_{-k+k_1}(t)\rangle=\int dy' e^{-i(p-k_1)y'}I_{-k+k_1}(y',t). \tag{B8}$$

Inserting this expression into the first term on the right-hand side of Eq. (B7) gives

$$\begin{aligned}
&=i\int dk_1dy'dpk_1e^{i(y-y')p}e^{ik_1y'}I_{-k+k_1}(y',t)\int dx\phi_{k+p}^>(x) \\
&\times(1-\partial_{xx}+k_2^2)\partial_x\phi_{k_2}^>(x)\phi_{k_1}^<(x) \\
&=i\int dk_1dy'dpk_1e^{i(y-y')p}e^{ik_1y'}I_{-k+k_1}(y',t)\int dx\phi_{k+p}^>(x) \\
&\times(1-\partial_{xx}+k_2^2)\partial_x\phi_{k_2}^>(x)\phi_{k_1}^<(x).
\end{aligned} \tag{B9}$$

The other nonlinear terms can be treated similarly. It is now necessary to evaluate the spatial integrals. To lowest order, $\phi_{k_1}^{<}(x)$ may be treated as a constant and pulled out of the integral. However, since we are anticipating that the large scale mean fields vary strongly in the radial direction, we instead expand $\phi_{k_1}^{<}(x)$ about the r_{m_1,n_1} resonant surface. Keeping up to second order in the power series expansion for $\phi_{k_1}^{<}(x)$, and performing the spatial integrals gives

$$\frac{\partial}{\partial t}N_k+\frac{\partial}{\partial k}(\omega_k+\delta\omega_k)\frac{\partial}{\partial y}N_k-\frac{\partial}{\partial y}\delta\omega_k\frac{\partial}{\partial k}N_k = \gamma_k N_k - F[\phi^{<}]N_k-\Delta\omega_k N_k^2, \tag{B10}$$

$$\delta\omega_k=\frac{k\left[\left(1+k^2-\frac{1}{2}\mu_{ik}\right)\left(k^2-\frac{1}{2}\mu_{ik}\right)+\left(\frac{1}{4}\mu_{rk}\right)^2\right]}{\left(1+k^2-\frac{1}{2}\mu_{ik}\right)^2+\frac{1}{4}(\mu_{rk})^2}\frac{\partial\phi^{<}}{\partial x},$$

$$N_k=\left[\left(1+k^2-\frac{1}{2}\mu_{ik}\right)\left(k^2-\frac{1}{2}\mu_{ik}\right)+\frac{1}{4}\mu_{rk}^2\right]I_k,$$

$$F[\phi^{<}]=-\frac{\mu_{rk}\partial_x\phi^{<}}{\left(1+k^2-\frac{1}{2}\mu_{ik}\right)^2+\frac{1}{4}\mu_{rk}^2}+\left[(1+k^2)(k^2-3\mu_{ik})+\frac{3}{4}|\mu_k|^2\right]\frac{\mu_{rk}\partial_k r_k\partial_{yy}\phi^{<}}{\left(1+k^2-\frac{1}{2}\mu_{ik}\right)^2+\frac{1}{4}\mu_{rk}^2}+\frac{1}{2}\frac{k}{|\mu_k|^2}\left[k^2\left(1+k^2-\frac{1}{2}\mu_{ik}\right)-\frac{1}{4}|\mu_k|^2\right]\frac{\mu_{rk}\partial_{xxx}\phi^{<}}{\left(1+k^2-\frac{1}{2}\mu_{ik}\right)^2+\frac{1}{4}(\mu_{rk})^2}-\left[\frac{1}{2}\mu_{rk}^2+\left(1+k^2-\frac{1}{2}\mu_{ik}\right)\left(\mu_{ik}+\frac{1}{2}k\partial_k\mu_{ik}\right)-\frac{1}{4}k\mu_{rk}\partial_k\mu_{rk}\right]\times\frac{\partial_{xy}\phi^{<}}{\left(1+k^2-\frac{1}{2}\mu_{ik}\right)^2+\frac{1}{4}\mu_{rk}^2}+\frac{1}{2}\left(1+k^2-\frac{1}{2}\mu_{ik}\right)\frac{k\mu_{rk}\partial_k\mu_{rk}\partial_{xy}\phi^{<}}{\left[\left(1+k^2-\frac{1}{2}\mu_{ik}\right)^2+\frac{1}{4}\mu_{rk}^2\right]^2}.$$

Following a similar procedure as in the homogeneous case shown above (explained in detail in Ref. 46), Eq. (B10) can be linearized and inserted into Eq. (6). This allows the polarization nonlinearity in the vorticity equation for the large scales to be written as

$$\langle(\hat{\mathbf{z}}\times\nabla\phi^{>})\cdot\nabla\nabla_{\perp}^2\phi^{>}\rangle(\mathbf{x},t)=C(\mathbf{q})\phi^{<}. \tag{B11}$$

A plot of the structure of $C(\mathbf{q})$ is given in the following as a function of q_y and q_x for the parameters given by $T_e/T_i=2$, $\eta_i=15$, $a/L_s=q'/\epsilon=-1/8$, $R/a=1.6$, $\Gamma=5/3$, $\epsilon=a/R_m$, $\alpha=-3$, where a and R_m are the minor and major radii, respectively, and α, which is the exponent of the equilibrium wave action spectrum. (Fig. 7)

Here q_x and q_y should be interpreted as inverse radial length scales associated with the large scale mode. The dark portions of the graph correspond to negative values of $C(\mathbf{q})$. It is apparent that the above structures die off rapidly for large poloidal wave numbers (small poloidal scales), however the magnitude of $C(\mathbf{q})$ remains much more pronounced for large radial wave numbers (small radial scales). This leads one to expect strong excitation of poloidally extended, narrow radial structures, as is the case with a tearing mode or zonal flow.

[1] H. Wilson, J. Connor, R. Hastie, and C. Hegna, Phys. Plasmas **3**, 248 (1996).
[2] R. L. Haye, S. Gunter, D. Humphreys, J. Lohr, T. Luce, M. Maraschek, C. Petty, R. Prater, J. Scoville, and E. Strait, Phys. Plasmas **9**, 2051 (2002).
[3] A. Smolyakov, Plasma Phys. Controlled Fusion **35**, 657 (1993).
[4] C. Hegna, Phys. Plasmas **5**, 1767 (1998).
[5] Z. Chang, J. Callen, E. Fredrickson, R. Budny, C. Hegna, K. Mcguire, and M. Zarnstorff, Phys. Rev. Lett. **74**, 4663 (1995).
[6] R. Carrera, R. Hazeltime, and M. Kotschenreuther, Phys. Fluids **29**, 899 (1986).
[7] S. Cappello and D. Escande, Phys. Rev. Lett. **85**, 3838 (2000).
[8] X. Shan and D. Montgomery, Plasma Phys. Controlled Fusion **35**, 1019 (1993).
[9] A. Smolyakov, P. Diamond, and M. Malkov, Phys. Rev. Lett. **84**, 491 (2000).
[10] P. Kaw, R. Singh, and P. Diamond, Plasma Phys. Controlled Fusion **44**, 51 (2002).
[11] O. Gurcan, P. Diamond, T. Hahm, and Z. Lin, Phys. Plasmas **12**, 032303 (2005).
[12] T. Hahm, P. Diamond, Z. Lin, K. Itoh, and S.-I. Itoh, Plasma Phys. Controlled Fusion **46**, A323 (2004).
[13] Z. Lin and T. Hahm, Phys. Plasmas **3**, 1099 (2004).
[14] P. Kaw, E. Valeo, and P. Rutherford, Phys. Rev. Lett. **43**, 1398 (1979).
[15] H. Strauss, Phys. Fluids **29**, 3668 (1986).
[16] K. Itoh, S.-I. Itoh, and A. Fukuyama, Phys. Rev. Lett. **69**, 1050 (1992).

[17] P. Diamond, R. Hazeltine, Z. An, B. Carreras, and H. Hicks, Phys. Fluids **27**, 1449 (1984).
[18] S.-I. Itoh, K. Itoh, and M. Yagi, Plasma Phys. Controlled Fusion **46**, 123 (2004).
[19] M. Yagi, S. Yoshida, S.-I. Itoh, H. Naitou, H. Nagahara, J.-N. Leboeuf, K. Itoh, T. Matsumoto, S. Tokuda, and M. Azumi, Nucl. Fusion **45**, 900 (2005).
[20] R. Trines, R. Bingham, L. Silva, J. Mendonca, P. Shukla, and W. Mori, Phys. Rev. Lett. **94**, 165002 (2005).
[21] P. Diamond, S.-I. Itoh, K. Itoh, and T. Hahm, Plasma Phys. Controlled Fusion **47**, R35 (2005).
[22] A. Smolyakov and P. Diamond, Phys. Plasmas **6**, 4410 (1999).
[23] B. Dubrulle and S. Nazarenko, Physica D **110**, 123 (1997).
[24] A. Hasegawa and K. Mima, Phys. Fluids **21**, 87 (1978).
[25] I. Gruzinov, A. Das, P. Diamond, and A. Smolyakov, Phys. Lett. A **302**, 119 (2002).
[26] P. Guzdar, R. Kleva, A. Das, and P. Kaw, Phys. Rev. Lett. **87**, 015001 (2001).
[27] H. Furth, J. Killeen, and M. Rosenbluth, Phys. Fluids **6**, 459 (1963).
[28] A. Bondeson and J. Sobel, Phys. Fluids **27**, 2028 (1984).
[29] F. Porcelli, Phys. Fluids **30**, 1734 (1987).
[30] B. Carreras, M. Rosenbluth, and H. Hicks, Phys. Rev. Lett. **46**, 1131 (1981).
[31] P. Tabeling, Phys. Rep. **362**, 1 (2002).
[32] J. Connor, F. Waelbroeck, and H. Wilson, Phys. Plasmas **8**, 2835 (2001).
[33] P. Rutherford, Phys. Fluids **16**, 1903 (1973).
[34] M. Rosenbluth and F. Hinton, Phys. Rev. Lett. **80**, 724 (1998).
[35] K. Shaing, C. Hegna, J. Callen, and W. Houlberg, Nucl. Fusion **43**, 258 (2003).
[36] M. Pedrosa, C. Hidalgo, A. Lopez-Fraguas, B. V. Milligen, R. Balbin, J. Jimenez, E. Sanchez, J. Castellano, L. G. the TJ-II team, B. Carreras, *et al.*, Czech. J. Phys. **50**, 1463 (2000).
[37] L. Garcia, B. Carreras, V. Lynch, M. Pedrosa, and C. Hidalgo, Phys. Plasmas **8**, 4111 (2001).
[38] M. E. Austin, presented at the 47th APS-DPP Meeting, Denver, Colorado, 2005.
[39] K. Burrell, Phys. Plasmas **4**, 1499 (1997).
[40] J. Connor, T. Fukuda, X. Garbet, C. Gormezano, V. Mukhovatov, and M. Wakatani, Nucl. Fusion **44**, R1 (2004).
[41] Y. Kishimoto, J.-Y. Kim, W. Horton, T. Tajima, M. LeBrun, S. Dettrick, J. Li, and S. Shirai, Nucl. Fusion **40**, 667 (2000).
[42] C. Ritz, T. Rhodes, H. Lin, W. Rowan, A. Wootton, B. Carreras, J. Leboeuf, D. Lee, J. Holmes, J. Harris, *et al.*, *Proceedings of the 13th IAEA International Conference on Plasma Physics and Controlled Nuclear Fusion Research* (IAEA, Vienna 1991), Vol. 2, p. 589.
[43] J. Leboeuf, D. Lee, B. Carreras, N. Dominguez, and J. Harris, *et al.*, Phys. Fluids **29**, 3668 (1986).
[44] B. Carreras, K. Sidikman, P. Diamond, P. Terry, and L. Garcia, Phys. Fluids B **4**, 3115 (1992).
[45] G. Lee and P. Diamond, Phys. Fluids **29**, 3291 (1986).
[46] V. Lebedev, P. Diamond, V. Shapiro, and G. Soloviev, Phys. Plasmas **2**, 4420 (1995).